HHS Public Access

Author manuscript

J Immunol. Author manuscript; available in PMC 2019 February 01.

Published in final edited form as:

J Immunol. 2018 February 01; 200(3): 1188–1197. doi:10.4049/jimmunol.1700999.

Nlrp12 mediates adverse neutrophil recruitment during influenza virus infection

Emma E. Hornick[*], **Balaji Banoth**[†], **Ann M. Miller**[*], **Zeb R. Zacharias**[*,‡], **Nidhi Jain**[†], **Mary E. Wilson**[*,§,¶], **Katherine N. Gibson-Corley**[‡], **Kevin L. Legge**[*,‡,‖], **Gail A. Bishop**[*,§,¶,‖], **Fayyaz S. Sutterwala**[*,†,#], and **Suzanne L. Cassel**[*,†,#]

[*]Interdisciplinary Program in Immunology, University of Iowa Carver College of Medicine, Iowa City, IA 52242, USA

[†]Department of Medicine, Cedars-Sinai Medical Center, Los Angeles, CA 90048, USA

[‡]Department of Pathology, University of Iowa Carver College of Medicine, Iowa City, IA 52242, USA

[§]Department of Internal Medicine, University of Iowa Carver College of Medicine, Iowa City, IA 52242, USA

[¶]Veterans Affairs Medical Center, Iowa City, IA 52246, USA

[‖]Department of Microbiology & Immunology, University of Iowa Carver College of Medicine, Iowa City, IA 52242, USA

Abstract

Exaggerated inflammatory responses during influenza A virus (IAV) infection are typically associated with severe disease. Neutrophils are among the immune cells that can drive this excessive and detrimental inflammation. In moderation, however, neutrophils are necessary for optimal viral control. In this study, we explore the role of the nucleotide-binding domain leucine-rich repeat containing receptor (NLR) family member Nlrp12 in modulating neutrophilic responses during lethal IAV infection. *Nlrp12*$^{-/-}$ mice are protected from lethality during IAV infection and show decreased vascular permeability, fewer pulmonary neutrophils, and a reduction in levels of neutrophil chemoattractant CXCL1 in their lungs compared to wild-type (WT) mice. *Nlrp12*$^{-/-}$ neutrophils and dendritic cells (DCs) within the IAV-infected lungs produce less CXCL1 than their WT counterparts. Decreased CXCL1 production by *Nlrp12*$^{-/-}$ DCs was not due to a difference in CXCL1 protein stability, but instead to a decrease in *Cxcl1* mRNA stability. Together, these data demonstrate a previously unappreciated role for Nlrp12 in exacerbating the pathogenesis of IAV infection through the regulation of CXCL1 mediated neutrophilic responses.

Correspondence to: Suzanne L. Cassel, Cedars-Sinai Medical Center, 127 S. San Vicente Blvd, AHSP, Room A9402, Los Angeles, CA 90048; suzanne.cassel@cshs.org.

[#]These authors contributed equally to this work

Disclosures: The authors declare no conflicts of interest.

Introduction

Severe disease during influenza A virus (IAV) infection is associated with excessive cytokine production and an exaggerated innate immune response, leading to substantial tissue damage and impaired respiratory function (1-3). The heightened morbidity and mortality among otherwise healthy adults infected with the 2009 pandemic H1N1 strain emphasized the threat posed by emerging strains to which there is little or no pre-existing immunity in the population.

The presence of elevated neutrophil chemoattractants and massive neutrophil infiltration of the lungs in lethal cases of IAV suggested a detrimental role for neutrophils during IAV infection (1, 4, 5). Subsequent studies have revealed a much more nuanced relationship between neutrophils and the IAV-infected lung. Neutrophils are among the first immune cells to arrive in the lungs, where they contribute to viral clearance through phagocytosis of viral particles and IAV-infected apoptotic cells (6). Neutrophil depletion in mice during IAV infection results in increased viral titers and mortality (7, 8), however mice deficient in key neutrophil effector molecules such as myeloperoxidase or chemoattractants such as CXCL2 have less severe disease (9, 10). A recent study provided an excellent framework for understanding these dissonant results, finding that enhancement of inflammatory signaling networks driven largely by neutrophils is an early predictor of lethality (7, 11). Key effector molecules downstream of activation of these networks include neutrophil chemoattractants (CXCL1, 2 and 5) and their receptor (CXCR2). Partial depletion of neutrophils reduced mortality during lethal infection, supporting the notion that control of early inflammatory responses is key to survival in high dose infections (11).

Nlrp12 is a member of the nucleotide binding domain and leucine rich repeat containing receptor (NLR) family that has been implicated in regulation of pro-inflammatory signaling in the context of bacterial infections, tumorigenesis and autoimmunity (12-14). We and others have recently shown that Nlrp12-deficient cells produce decreased CXCL1, a potent neutrophil chemoattractant, during bacterial infections (13, 15). Given the complex role of neutrophils during IAV infection, we sought to determine whether Nlrp12 influenced host susceptibility to IAV infection. We report that *Nlrp12*$^{-/-}$ mice have significantly improved survival following IAV infection in comparison to wild-type (WT) mice. *Nlrp12*$^{-/-}$ mice maintained their ability to control infection and have decreased CXCL1-driven pulmonary vascular permeability and pulmonary neutrophil recruitment.

Materials and Methods

Mice

The generation of *Nlrp12*$^{-/-}$ mice has been described elsewhere (16). Mice were backcrossed to C57BL/6N or BALB/cJ mice for at least nine generations and maintained in an SPF facility. C57BL/6N mice were purchased from the Charles River Laboratories and used as WT controls unless otherwise stated; BALB/cJ and C57BL/6J mice were purchased from the Jackson Laboratories. Both male and female mice 6-10 weeks of age were used, however mice were sex-, age-, and weight-matched for individual experiments. The Institutional

Animal Care and Use Committee at the University of Iowa approved all protocols used in this study.

Virus and *in vivo* infection

Mouse-adapted IAV strain A/PR/8/34 was propagated as previously described (17). Mice were anesthetized with ketamine and xylazine and infected intranasally with virus diluted in 50μL sterile DMEM. Weight was monitored daily and mice were euthanized upon losing 30% of their starting weight. For CXCL1 blocking experiments, mice were administered 5μg anti-CXCL1 (MAB453, clone 48415, R&D Systems) or isotype control antibody i.p. immediately prior to infection and 24 and 72 hours after infection.

Lung titers, Sectioning, and Histology

To measure virus titers, lungs were homogenized using a TissueTearor (Biospec), then homogenates were clarified by centrifugation and immediately frozen at -80°C. A standard plaque assay on MDCK cells was subsequently used to quantify infectious virus. For histology, lungs were fixed in 10% neutral buffered formalin, embedded, cut at 5μm and stained with hematoxylin and eosin (H&E). A single H&E-stained slide from each of 5 separate animals per group was evaluated by a board-certified veterinary pathologist in a blinded fashion and both necrosis and pulmonary inflammation were assessed using semi-quantitative scoring. Necrosis score: necrosis was defined by cellular necrosis of the bronchiolar epithelial cells and/or the pneumocytes, which was accompanied by accumulation of necrotic cellular debris in these regions. The entire slide was evaluated and included both the right and left lung lobes. 0 = no necrosis; 1 = rare (1-3) scattered areas of necrosis throughout the lung; 2 = multifocal (3-9) scattered areas of necrosis throughout the lung; 3 = numerous (greater than 10) areas of necrosis throughout the lung. Inflammation score: Inflammation was defined by the accumulation of inflammatory cells, primarily viable and degenerate neutrophils, within airways and/or alveolar spaces. 0 = no inflammation; 1 = 1-10% of the pulmonary parenchyma contains inflammatory cell infiltrates; 2 = 10-50% of the pulmonary parenchyma contains inflammatory cell infiltrates; 3 = >50% the pulmonary parenchyma contains inflammatory cell infiltrates.

ELISA

Cytokines and chemokines were quantified in cell culture supernatants and lung homogenate supernatants using DuoSet mouse ELISA kits from R&D Systems: CXCL1, CXCL2, CXCL5, IL-1β, CCL2 and CCL5; or ReadySetGo! mouse ELISA kits from eBioscience: IL-6, TNFα, IL-10, IL-1α, IL-12p40, and IFNγ following manufacturer's instructions.

Flow cytometry

For some experiments, intravascular staining for CD45.2 was performed as described (18) prior to tissue harvest. Single cell suspensions were prepared by pressing tissues through wire mesh screens. Live cells were enumerated by Trypan blue exclusion. 1×10^6 cells per well were blocked with 2% rat serum and anti-mouse CD16/32 (clone 2.4G2, Tonbo Biosciences) in FACS Buffer for 30 minutes at 4°C. Following blocking, cells were stained in FACS buffer with fluorochrome-conjugated antibodies in the dark for 30 minutes at 4°C.

Cells were then fixed in FACS Lysis Buffer (BD) per manufacturer's instructions and resuspended in PBS. The following fluorochrome-conjugated antibodies were used: CD4 (clone GK1.5), CD8a (53-6.7), CD11a (M17/4), CD11b (M1/70), CD45.2 (104), CD49d (R1-2), CD64 (X54-5/7.1FC), CD90.2 (30-H12), Ly6G (1A8), Ly6C (HK1.4), and I-A/I-E (M5/114.15.2) from Biolegend; CD4 (RM4-5) from eBioscience; and CD11c (HL3) from BD Biosciences. Data was acquired on a BD LSR II and analyzed with FlowJo software (FlowJo, LLC). For detection of intracellular CXCL1, mice were treated with 500μg monensin (Sigma) i.p. five hours prior to harvest to inhibit cytokine/chemokine secretion. Tissue processing and surface staining was performed as above, but 0.1mg/mL monensin and 5μg/mL Brefeldin A (Sigma) were present in all solutions until fixation. Cells were fixed, permeabilized and stained using Transcription Factor Staining Kit (eBioscience) according to the manufacturer's instructions. CXCL1 was detected by biotinylated anti-CXCL1 (R&D Systems, BAF453) and APC-labeled streptavidin (eBioscience). Live cells were sorted for gene expression analysis on a BD FACS Aria II. Hoechst dye was added to cells prior to sorting to identify live cells, which were collected and processed for gene expression analysis (as below) after sorting.

Microvascular permeability

We assessed microvascular permeability by extravasation of Evans blue dye as previously described (19). Briefly: mice were injected i.v. with 20mg/kg Evans blue dye. One hour later, lungs were perfused with PBS, weighed, and homogenized. Evans blue dye in lung homogenates was extracted with formamide (Sigma) at 60°C for 18 hours. Absorbance of lung homogenate supernatants at 620nm and 740nm was measured to calculate μg Evans blue dye per g lung tissue.

In vitro infection and stimulation of bone marrow-derived cells

Bone marrow-derived dendritic cells (BMDCs) and macrophages (BMMs) were generated as described (13, 20). Bone marrow neutrophils were purified by negative selection with an EasySep Mouse Neutrophil Enrichment Kit (Stemcell Technologies), following manufacturer's instructions. On day six of culture, 1×10^6 BMDCs were infected with IAV (MOI=5) in serum-free infection medium for 60 minutes, then washed twice with PBS and incubated in complete medium until harvest. Alternatively, BMDCs were treated with 1μg/mL R848 (Invivogen) in complete medium until harvest. For transcript stability experiments, 10μg/mL Actinomycin D (Sigma) was added to BMDCs, BMMs or neutrophils after three hours of 1μg/mL R848 stimulation. For protein stability experiments, 10μg/mL Cyclohexamide (Sigma) was added to BMDCs after six hours of R848 stimulation. To assess neutrophil death, freshly isolated neutrophils were incubated with 30ng/mL Phorbol 12-myristate 13-acetate (PMA, Sigma), 4ng/mL CXCL1 (#250-11, Peprotech) or in complete medium until harvest. Incubation with IAV was performed as for BMDCs (see above).

Gene expression analysis

RNA was extracted using the RNeasy Plus Mini Kit (Qiagen) per manufacturer's instructions. cDNA was synthesized using Superscript III First Strand Synthesis SuperMix (Invitrogen). qPCR was performed using cDNA, primer pairs for *Cxcl1*, *Il6*, and *Actb*

(Qiagen PPM03058C, PPM03015A, and PPM02945B), and PerfeCta SYBR Green Fastmix (Quanta Biosciences). Reactions were run in a QuantStudio 6 Flex (Applied Biosystems) with a standard cycling protocol (90°C 2min; 40 cycles of 95°C 15sec, 60°C 1min). qPCR data were analyzed using the $2^{-\Delta\Delta Ct}$ method where ΔΔCt = [(Ct gene of interest-Ct housekeeping) stimulated – (Ct gene of interest-Ct housekeeping) unstimulated]. *Actb* was chosen as a housekeeping gene.

Western Blotting

Lysates were prepared in RIPA buffer (Cell Signaling Technologies) with 1mM PMSF per manufacturer's instructions. Proteins were separated on a NuPAGE gel (Invitrogen) and transferred to a PVDF membrane using the XCell II blotting system (Invitrogen). Membranes were blocked with 5% nonfat milk and incubated with primary antibody overnight at 4°C. Primary antibodies were purchased from Cell Signaling Technologies: IRAK1 (#4504), phospho-IkBa (#2859), IkBa (#4814), phospho-p38 MAPK (#4511), p38 MAPK (#8690), phospho-p44/42 MAPK (ERK1/2, #4370), p44/p42 MAPK (ERK1/2, #4695), NFkB2 p100/p52 (#4882), phospho-NFkB p65 (#3033), NFkB p65 (#8242) phospho-TBK1 (#5483), TBK1 (#3504). CXCL1 (PA1-29220, Thermo Fisher Scientific), GAPDH (CB1001), and total actin antibody (MAB1501) were purchased from EMD Millipore. HuR (sc-5261), IRAK1 (sc-5288), phospho-MAPKAPK2 (sc-293139), MAPKAPK2 (sc-393609), and TTP (sc-374305) were purchased from Santa Cruz Biotechnology. TRAF2 (592) was purchased from Medical & Biological Laboratories. Following washing, membranes were incubated with HRP-tagged anti-mouse IgG (1706516, Bio-Rad) or anti-rabbit IgG (NA934, GE Healthcare) and developed using SuperSignal West Pico or Femto substrate (Thermo Fisher Scientific).

Statistics

Data were graphed and indicated statistical tests performed using GraphPad Prism software.

Results

Nlrp12 deficiency improves survival following IAV infection

To determine whether Nlrp12 is important for protection during a high-dose IAV infection, we infected WT C57BL/6N and *Nlrp12*$^{-/-}$ mice with a $4LD_{50}$ inoculum of IAV and monitored survival and weight loss as a measure of morbidity. Strikingly, 67% of *Nlrp12*$^{-/-}$ mice survived the infection, compared with 0% survival in the WT group at day 14 post-infection (Fig. 1A). Apart from a failure of WT mice to regain weight after day 10, no significant differences in weight loss were apparent (Fig. 1A). Similar results were observed in *Nlrp12*$^{-/-}$ mice backcrossed onto a BALB/c background (Supplementary Fig. S1A).

T cell responses are critical for protection during a primary IAV infection, and augmentation of the $CD8^+$ T cell response during high dose infections improves survival (17). A recent study suggested that *Nlrp12*$^{-/-}$ $CD4^+$ and $CD8^+$ T cells exhibit increased expansion and pro-inflammatory cytokine production upon stimulation (12), prompting us to investigate the possibility that *Nlrp12*$^{-/-}$ mice had enhanced T cell responses during high-dose IAV infection. Interestingly, we found no difference in the magnitude of the IAV-specific $CD8^+$

or $CD4^+$ T cell responses (Fig. 1B, C and S1B, C)(21). Consistent with the importance of IAV-specific $CD8^+$ T cells for viral clearance, we observed no difference in virus titers in the lungs of WT and *Nlrp12*$^{-/-}$ mice at day three or seven post-infection (Fig. 1D). Histopathologic analysis indicated more pathology overall in the lungs of WT mice than *Nlrp12*$^{-/-}$ mice at day five post-infection, with increased hemorrhage and necrotic debris in airways and alveoli (Fig. 1E, F).

Nlrp12 modulates CXCL1 during IAV infection

Unrestrained pro-inflammatory cytokine production is a hallmark of severe disease during IAV infections in humans and mice (2). Although IL-1β, IL-6 and TNFα are closely associated with disease severity and weight loss we saw no significant differences in the amount of these cytokines at early or late time points in the lungs of WT and Nlrp12-deficient mice (Fig. 2A-C). In contrast, neutrophil chemoattractant CXCL1 was dramatically reduced in *Nlrp12*$^{-/-}$ mice compared to WT mice at day three but not day seven post-infection (Fig. 2D). Neutrophil chemoattractants CXCL2 and CXCL5 were not different between the two groups, nor were a number of other cytokines and chemokines involved in inflammation and recruitment of innate and adaptive immune cells (Fig. 2E, F and S1D-I). Therefore *Nlrp12*$^{-/-}$ mice have a specific reduction in pulmonary CXCL1 during the early phase of IAV infection.

Nlrp12$^{-/-}$ mice have decreased pulmonary neutrophils

Neutrophils contribute to both viral clearance and immunopathology during IAV infection (7). They are recruited to the lungs early and peak three to five days after lethal PR8 infection (8). Following IAV infection we assessed inflammatory cell infiltration into the lung by flow cytometry (Fig. 3 and S2). At day three post-infection, we found that pulmonary neutrophils were significantly decreased, both in absolute number and percentage, in the lungs of *Nlrp12*$^{-/-}$ mice compared to WT (Fig. 3 and S2B). Intravascular staining revealed no difference in the percentage of neutrophils present in the lung vasculature of *Nlrp12*$^{-/-}$ mice compared to WT (Fig. S2B). This difference in pulmonary neutrophils was still present at days five and seven post infection, but we observed no significant differences in the number of macrophages, monocytes or DCs at any of the time points measured (Fig. 3 and S2B). The significant increases in the frequency of DCs and macrophages at days five and seven post-infection are due to the decreased total number of hematopoietic cells, and do not likely represent compensatory recruitment of these cells to the lungs (Fig. S2B). Previous studies have shown that IAV accelerates apoptosis in human neutrophils (22). We were interested to determine whether a difference in survival contributes to the decrease in neutrophils present in the IAV-infected lungs of *Nlrp12*$^{-/-}$ mice. We quantified neutrophil death following incubation with IAV, CXCL1, or PMA and found no increase in death among *Nlrp12*$^{-/-}$ neutrophils compared to WT neutrophils (Fig. S2C). Therefore, increased death of neutrophils in the lungs of *Nlrp12*$^{-/-}$ mice is not likely to be driving the decrease in those cells in the lungs following IAV infection. We further quantified pulmonary neutrophil recruitment in littermate *Nlrp12*$^{+/+}$, *Nlrp12*$^{+/-}$ and *Nlrp12*$^{-/-}$ mice following infection with IAV and found that both *Nlrp12*$^{+/-}$ and *Nlrp12*$^{-/-}$ mice had significantly fewer pulmonary neutrophils than *Nlrp12*$^{+/+}$ mice (Fig. 4A, B), suggesting haploinsufficiency. We also compared neutrophil numbers in the lungs of IAV-infected

C57BL/6N and C57BL/6J substrains as C57BL/6J mice carry a missense mutation in *Nlrp12* (13, 23). Consistent with our findings in the context of bacterial infection, C57BL/6J mice had significantly fewer infiltrating pulmonary neutrophils compared to C57BL/6N mice three days after IAV infection (Fig. 4C, D). Together, these results strongly support a role for Nlrp12 in modulating pulmonary neutrophil accumulation during IAV infection.

Nlrp12$^{-/-}$ mice have decreased vascular permeability during IAV infection

Pulmonary edema due to diminished barrier integrity in IAV-infected lungs is a serious consequence of both the viral infection and the resultant immune response and is associated with increased mortality (24). Neutrophil-derived reactive oxygen species and cytokines have been implicated in epithelial-endothelial barrier damage during IAV infections (25). The observed decrease in pulmonary neutrophils in *Nlrp12*$^{-/-}$ mice led us to ask whether there would also be less pulmonary vascular permeability in *Nlrp12*$^{-/-}$ mice compared to WT mice. Utilizing Evans blue dye extravasation as an indicator of vascular permeability we found that at day five post-infection *Nlrp12*$^{-/-}$ mice had significantly decreased vascular permeability compared to WT mice (Fig. 5A).

Binding of CXCL1 to CXCR2 on endothelial cells increases microvascular permeability in the lungs (26). When a CXCL1 blocking antibody was administered to WT mice during IAV infection, vascular permeability and pulmonary neutrophils, but not DCs or macrophages, were decreased at day five post-infection (Fig. 5B-E) similar to our findings with *Nlrp12*$^{-/-}$ mice. Therefore, Nlrp12-dependent modulation of CXCL1 levels plays a role in vascular permeability during IAV infection.

Cellular source of CXCL1 in the lungs during IAV infection

We next determined the cellular source of CXCL1 in IAV-infected lungs. We treated IAV-infected mice with monensin to prevent cells from secreting CXCL1, then assessed intracellular CXCL1 by flow cytometry. We found that a higher percentage of CD45.2^{+} hematopoietic cells than CD45.2^{-} non-hematopoietic cells were CXCL1^{+}, and there was no significant difference in the proportion of CXCL1^{+} non-hematopoietic cells between WT and *Nlrp12*$^{-/-}$ mice (Fig. 6A, B). Among immune cell subsets, the frequency of CXCL1^{+} neutrophils and DCs was significantly decreased in *Nlrp12*$^{-/-}$ mice, but there was no difference in the proportion of CXCL1^{+} macrophages at day two or three post-infection (Fig. 6C). To determine whether the decrease in CXCL1 was due to a change in *Cxcl1* transcription, we sorted the same cell populations from IAV-infected lungs and measured *Cxcl1* transcript levels. We found decreased *Cxcl1* message in DCs and neutrophils at day two post-infection, and decreased *Cxcl1* message in DCs, neutrophils and macrophages at day three post-infection (Fig. 6D).

Nlrp12 is highly expressed in neutrophils, moderately expressed in bone marrow-derived dendritic cells, and only modestly expressed in bone marrow-derived macrophages (16). We therefore determined the relative expression of *Nlrp12* in CXCL1-producing subsets of cells in the IAV-infected lung. Consistent with published data, we found that neutrophils had the greatest expression of *Nlrp12* at days two and three post-infection, over 10x more than in

DCs and 100x more than in macrophages (Fig. 6E). Together, these data demonstrate that both *Nlrp12* and *Cxcl1* are highly expressed in hematopoietic cells.

Decreased *Cxcl1* mRNA stability in *Nlrp12*$^{-/-}$ BMDCs

Induction of *Cxcl1* can occur downstream of NFκB activation, and previous studies have implicated Nlrp12 in the regulation of NFκB activation (14, 27, 28). We therefore infected BMDCs with IAV and performed immunoblotting to assess activation of NFκB and MAPK family members. Interestingly, we found no pronounced differences in activation of NFκB or MAPK family members, despite decreased CXCL1 production by IAV-infected *Nlrp12*$^{-/-}$ BMDCs (Fig. S3A-C). These data indicated that although the decrease in CXCL1 production by DCs in IAV-infected lungs is recapitulated in IAV-infected *Nlrp12*$^{-/-}$ BMDCs, this is unlikely due to alterations in signaling pathways that ultimately converge on *Cxcl1* transcription.

IAV does not robustly infect BMDCs (29), thus it was possible that sub-optimal or asynchronous stimulation of virus-sensing PRRs was obscuring signaling differences. To circumvent this, we treated BMDCs with the TLR7 agonist R848 and again observed decreased CXCL1, but not IL-6, protein and mRNA in *Nlrp12*$^{-/-}$ compared to WT BMDCs (Fig. 7A-D). Similar to results from IAV infection we again did not see any differences in activation of NFκB or MAPK family members between WT and *Nlrp12*$^{-/-}$ BMDCs following challenge with R848, nor did we see any difference in CXCL1 protein stability (Fig. S3D-F).

Given a lack of evidence for alterations in signaling pathways that culminate in transcription of pro-inflammatory mediators including CXCL1, we next investigated the possibility that *Cxcl1* mRNA stability was different in *Nlrp12*$^{-/-}$ BMDCs compared with WT BMDCs. We measured *Cxcl1* and *Il6* transcript decay by qRT-PCR in R848-treated BMDCs following transcription blockade with Actinomycin D (ActD). Interestingly, we found an increased rate of *Cxcl1* transcript decay in *Nlrp12*$^{-/-}$ BMDCs compared to WT BMDCs, whereas the rate of *Il6* transcript decay was unchanged (Fig. 7E, F). The half-life of *Cxcl1* transcript was approximately 30 minutes longer in WT BMDCs than in *Nlrp12*$^{-/-}$ BMDCs, but no difference in *Cxcl1* transcript stability was observed in bone marrow-derived macrophages or neutrophils (Fig S4A, B). Together, these data suggest that Nlrp12 plays a role in *Cxcl1* transcript stability specifically in BMDCs.

Stability of transcripts including *Cxcl1, Il6* and *Tnf* can be modulated through conserved AU-rich elements (AREs) in their 3′ UTRs (30, 31). ARE binding proteins mediate the regulatory function of AREs by stabilizing or destabilizing specific mRNAs in response to upstream signaling, commonly from PRRs or cytokine receptors. *Cxcl1* mRNA is present at very low levels in resting myeloid cells, reflecting that the continuous transcription of *Cxcl1* is followed by the binding of these transcripts by the ARE-binding protein tristetraprolin (TTP), that leads to transcript degradation. Upon stimulation of macrophages with LPS, *Cxcl1* transcription increases and the mRNA is stabilized in part via p38 MAPK and MAPKAPK2-mediated phosphorylation of TTP, which affects its cellular localization and ability to recruit degradation machinery to the mRNA(30). Under different stimulatory conditions, stabilizing (HuR) and destabilizing factors (SF2 via TRAF2/5 and Act1, KSRP)

affect the abundance of *Cxcl1* mRNA (32). We thus asked if the regulation of *Cxcl1* mRNA by Nlrp12 involved one of these pathways. WT and *Nlrp12*$^{-/-}$ BMDCs were stimulated with R848 followed by immunoblotting for ARE-binding and associated proteins. We found no differences in the abundance or activation of any of these proteins, nor did we see a difference in activation of translation initiation factor eIF4E (Fig. S4C). Together, these data indicate that the mechanism by which Nlrp12 affects *Cxcl1* transcript stability in BMDCs is likely through pathways distinct from those that have been described downstream of either LPS or cytokine stimulation.

Discussion

This work demonstrates that Nlrp12 contributes to disease severity during IAV infection through its effect on CXCL1 production, neutrophil recruitment to the lungs, and vascular permeability. Our finding that *Nlrp12*$^{-/-}$ mice have decreased—but not ablated—pulmonary neutrophils and improved survival is important because it supports a protective effect of neutrophils during IAV infection that is dependent on the magnitude of the neutrophilic response. We report a 25-40% decrease in the number of pulmonary neutrophils during infection, and show that this curtails enough of the immunopathology driven by excessive innate inflammatory responses without negatively affecting viral clearance or $CD8^+$ T cell responses, to result in improved survival. We also show that treatment with CXCL1-blocking antibody results in decreased neutrophil recruitment and decreased vascular permeability, consistent with the notion that down-modulation of early inflammatory mediators decreases disease severity.

The specific decrease in CXCL1 has broad implications for the overall course of disease due to direct and indirect effects on barrier function in the IAV-infected lung. The main complication of IAV infection is viral pneumonia, which can lead to acute respiratory distress syndrome (ARDS), respiratory failure, and death (24). Respiratory failure is precipitated by damage to the epithelial-endothelial barrier in the alveolus, which allows accumulation of proteinaceous fluid and immune cells that dramatically impair efficient gas exchange. CXCL1 can affect the barrier in at least two ways: first, by binding to CXCR2 on endothelial cells, causing retraction of the endothelial cells to increase microvascular permeability (26); second, by attracting CXCR2-expressing neutrophils to the site of infection, where they have the capacity to directly damage the epithelial cells in the lungs in the course of fighting infection (11). Thus, the decrease in CXCL1 observed in *Nlrp12*$^{-/-}$ animals may be protective to both sides of this critical barrier in the lung, ultimately lessening disease severity.

An important avenue of study will be to determine the mechanism by which Nlrp12 deficiency affects CXCL1 production. A recent study reported that CXCL1, CXCL5, IL-17A and neutrophil recruitment were decreased in *Nlrp12*$^{-/-}$ mice during pulmonary *Klebsiella pneumoniae* infection (15). Signaling through IL-17R leads to stabilization of *Cxcl1* and *Cxcl5* mRNA (32), which may explain the decrease observed during *K. pneumoniae* infection. However, IL-17A was not detected in the lungs of WT or *Nlrp12*$^{-/-}$ mice during IAV infection, thus it is unlikely to be driving the observed decrease in *Cxcl1* transcript stability. It is particularly intriguing that we observe a defect in CXCL1, and not

other neutrophil chemoattractants or pro-inflammatory mediators with similar patterns of transcriptional regulation. It is well established that modulation of neutrophil chemoattractant transcript stability is an important determinant of both the duration and magnitude of their expression, and that ARE-mediated instability is a key regulatory mechanism. Despite this generality, it is also clear that the precise regulation of the production of the chemokine reflects not only which gene is being regulated, but also varies according to the cell type in which the gene is being expressed as well as by the specific conditions under which that cell is being stimulated. Differential regulation of TNFα is illustrative of this mechanistic heterogeneiety: *Tnf* mRNA is stabilized following LPS stimulation of macrophages, resulting in increased expression, but following stimulation of macrophages through TLR7 or TLR9, upregulation is not through modification of transcript stability but rather occurs at the level of translation (33). Given this highly variant regulation and the fact that most studies of *Cxcl1* stability in myeloid cells have been performed in LPS-treated macrophages, it is not unexpected that a separate pathway would act to specifically modify *Cxcl1* transcript stability in BMDCs in response to R848 stimulation.

The importance of host genetic background to outcome during IAV infection has been demonstrated in a number of studies (34). Large-scale efforts such as the collaborative cross that seek to mimic the genetic diversity found in the human population are validating the importance of specific genes and discovering new correlates of protection (35). To our knowledge, there has not been a direct comparison of C57BL/6N and C57BL/6J substrains during IAV infection. The data presented here indicate that there is a significant reduction in the number of pulmonary neutrophils in the lungs of C57BL/6J mice compared to C57BL/6N mice following IAV infection. In the context of these data and our previous work, we believe this difference in neutrophil recruitment is due to the missense mutation in *Nlrp12* in C57BL/6J mice (13, 23), which phenocopies the neutrophil recruitment defect in *Nlrp12*$^{-/-}$ mice. This substantial phenotypic difference between substrains highlights the importance of ensuring that findings in knockout mice are confirmed using substrain-matched controls or littermates when possible.

In conclusion, the experiments described here show that *Nlrp12*$^{-/-}$ mice are protected from lethality during IAV infection, exhibiting less pulmonary microvascular permeability, CXCL1 and neutrophil recruitment. Modulation of the innate immune response to IAV is being increasingly appreciated as a key early intervention with durable protective effects. Our findings add Nlrp12 to the intracellular PRRs that contribute to early inflammatory responses during IAV infection.

Supplementary Material

Refer to Web version on PubMed Central for supplementary material.

Acknowledgments

The authors are grateful to members of the Inflammation Program, Eric Elliott, Bruce Hostager, Nurbek Mambetsariev, Alexis Miller, Diogo Valadares, and Alicia Wallis for valuable discussions and technical assistance. We also thank Tamara Mirzapoiazova for her generosity with microvascular permeability-related protocols and the University of Iowa Flow Cytometry Facility, a Carver College of Medicine / Holden Comprehensive Cancer Center core research facility, as well as the University of Iowa Comparative Pathology Laboratory, for their expertise.

NIH grants R01 AI118719 (F.S.S.), R01 AI104706 (S.L.C.), and an American Lung Association/AAAAI Foundation grant (S.L.C.) supported this work. E.E.H. received support from T32 AI007485 (G.A.B.).

References

1. Perrone LA, Plowden JK, García-Sastre A, Katz JM, Tumpey TM. H5N1 and 1918 Pandemic Influenza Virus Infection Results in Early and Excessive Infiltration of Macrophages and Neutrophils in the Lungs of Mice. PLoS Path. 2008; 4:e1000115.
2. Teijaro JR. The role of cytokine responses during influenza virus pathogenesis and potential therapeutic options. Curr Top Microbiol Immunol. 2015; 386:3–22. [PubMed: 25267464]
3. Iwasaki A, Pillai PS. Innate immunity to influenza virus infection. Nat Rev Immunol. 2014; 14:315–328. [PubMed: 24762827]
4. Narasaraju T, Yang E, Samy RP, Ng HH, Poh WP, Liew AA, Phoon MC, van Rooijen N, Chow VT. Excessive Neutrophils and Neutrophil Extracellular Traps Contribute to Acute Lung Injury of Influenza Pneumonitis. The American Journal of Pathology. 2011; 179:199–210. [PubMed: 21703402]
5. Ramos I, Fernandez-Sesma A. Modulating the Innate Immune Response to Influenza A Virus: Potential Therapeutic Use of Anti-Inflammatory Drugs. Front Immunol. 2015; 6:361. [PubMed: 26257731]
6. Hashimoto Y, Moki T, Takizawa T, Shiratsuchi A, Nakanishi Y. Evidence for phagocytosis of influenza virus-infected, apoptotic cells by neutrophils and macrophages in mice. J Immunol. 2007; 178:2448–2457. [PubMed: 17277152]
7. Tate MD, Ioannidis LJ, Croker B, Brown LE, Brooks AG, Reading PC. The role of neutrophils during mild and severe influenza virus infections of mice. PLoS One. 2011; 6:e17618. [PubMed: 21423798]
8. Tate MD, Deng YM, Jones JE, Anderson GP, Brooks AG, Reading PC. Neutrophils ameliorate lung injury and the development of severe disease during influenza infection. J Immunol. 2009; 183:7441–7450. [PubMed: 19917678]
9. Sugamata R, Dobashi H, Nagao T, Yamamoto K, Nakajima N, Sato Y, Aratani Y, Oshima M, Sata T, Kobayashi K, Kawachi S, Nakayama T, Suzuki K. Contribution of neutrophil-derived myeloperoxidase in the early phase of fulminant acute respiratory distress syndrome induced by influenza virus infection. Microbiol Immunol. 2012; 56:171–182. [PubMed: 22211924]
10. Sakai S, Kawamata H, Mantani N, Kogure T, Shimada Y, Terasawa K, Sakai T, Imanishi N, Ochiai H. Therapeutic effect of anti-macrophage inflammatory protein 2 antibody on influenza virus-induced pneumonia in mice. J Virol. 2000; 74:2472–2476. [PubMed: 10666283]
11. Brandes M, Klauschen F, Kuchen S, Germain Ronald N. A Systems Analysis Identifies a Feedforward Inflammatory Circuit Leading to Lethal Influenza Infection. Cell. 2013; 154:197–212. [PubMed: 23827683]
12. Lukens JR, Gurung P, Shaw PJ, Barr MJ, Zaki MH, Brown SA, Vogel P, Chi H, Kanneganti TD. The NLRP12 Sensor Negatively Regulates Autoinflammatory Disease by Modulating Interleukin-4 Production in T Cells. Immunity. 2015; 42:654–664. [PubMed: 25888258]
13. Ulland TK, Jain N, Hornick EE, Elliott EI, Clay GM, Sadler JJ, Mills KA, Janowski AM, Volk AP, Wang K, Legge KL, Gakhar L, Bourdi M, Ferguson PJ, Wilson ME, Cassel SL, Sutterwala FS. Nlrp12 mutation causes C57BL/6J strain-specific defect in neutrophil recruitment. Nat Commun. 2016; 7:13180. [PubMed: 27779193]
14. Allen IC, Wilson JE, Schneider M, Lich JD, Roberts RA, Arthur JC, Woodford RM, Davis BK, Uronis JM, Herfarth HH, Jobin C, Rogers AB, Ting JP. NLRP12 suppresses colon inflammation and tumorigenesis through the negative regulation of noncanonical NF-kappaB signaling. Immunity. 2012; 36:742–754. [PubMed: 22503542]
15. Cai S, Batra S, Del Piero F, Jeyaseelan S. NLRP12 modulates host defense through IL-17A-CXCL1 axis. Mucosal Immunol. 2016; 9:503–514. [PubMed: 26349659]
16. Arthur JC, Lich JD, Ye Z, Allen IC, Gris D, Wilson JE, Schneider M, Roney KE, O'Connor BP, Moore CB, Morrison A, Sutterwala FS, Bertin J, Koller BH, Liu Z, Ting JP. Cutting edge: NLRP12 controls dendritic and myeloid cell migration to affect contact hypersensitivity. J Immunol. 2010; 185:4515–4519. [PubMed: 20861349]

17. Legge KL, Braciale TJ. Lymph node dendritic cells control CD8+ T cell responses through regulated FasL expression. Immunity. 2005; 23:649–659. [PubMed: 16356862]

18. Anderson KG, Mayer-Barber K, Sung H, Beura L, James BR, Taylor JJ, Qunaj L, Griffith TS, Vezys V, Barber DL, Masopust D. Intravascular staining for discrimination of vascular and tissue leukocytes. Nat Protoc. 2014; 9:209–222. [PubMed: 24385150]

19. Moitra J, Sammani S, Garcia JG. Re-evaluation of Evans Blue dye as a marker of albumin clearance in murine models of acute lung injury. Transl Res. 2007; 150:253–265. [PubMed: 17900513]

20. Helft J, Bottcher J, Chakravarty P, Zelenay S, Huotari J, Schraml BU, Goubau D, Reis e Sousa C. GM-CSF Mouse Bone Marrow Cultures Comprise a Heterogeneous Population of CD11c(+)MHCII(+) Macrophages and Dendritic Cells. Immunity. 2015; 42:1197–1211. [PubMed: 26084029]

21. McDermott DS, Varga SM. Quantifying antigen-specific CD4 T cells during a viral infection: CD4 T cell responses are larger than we think. J Immunol. 2011; 187:5568–5576. [PubMed: 22043009]

22. Colamussi ML, White MR, Crouch E, Hartshorn KL. Influenza A virus accelerates neutrophil apoptosis and markedly potentiates apoptotic effects of bacteria. Blood. 1999; 93:2395–2403. [PubMed: 10090951]

23. Simon MM, Greenaway S, White JK, Fuchs H, Gailus-Durner V, Wells S, Sorg T, Wong K, Bedu E, Cartwright EJ, Dacquin R, Djebali S, Estabel J, Graw J, Ingham NJ, Jackson IJ, Lengeling A, Mandillo S, Marvel J, Meziane H, Preitner F, Puk O, Roux M, Adams DJ, Atkins S, Ayadi A, Becker L, Blake A, Brooker D, Cater H, Champy MF, Combe R, Danecek P, di Fenza A, Gates H, Gerdin AK, Golini E, Hancock JM, Hans W, Holter SM, Hough T, Jurdic P, Keane TM, Morgan H, Muller W, Neff F, Nicholson G, Pasche B, Roberson LA, Rozman J, Sanderson M, Santos L, Selloum M, Shannon C, Southwell A, Tocchini-Valentini GP, Vancollie VE, Westerberg H, Wurst W, Zi M, Yalcin B, Ramirez-Solis R, Steel KP, Mallon AM, de Angelis MH, Herault Y, Brown SD. A comparative phenotypic and genomic analysis of C57BL/6J and C57BL/6N mouse strains. Genome Biol. 2013; 14:R82. [PubMed: 23902802]

24. Short KR, Kroeze EJ, Fouchier RA, Kuiken T. Pathogenesis of influenza-induced acute respiratory distress syndrome. Lancet Infect Dis. 2014; 14:57–69. [PubMed: 24239327]

25. Snelgrove RJ, Edwards L, Rae AJ, Hussell T. An absence of reactive oxygen species improves the resolution of lung influenza infection. Eur J Immunol. 2006; 36:1364–1373. [PubMed: 16703568]

26. Reutershan J, Morris MA, Burcin TL, Smith DF, Chang D, Saprito MS, Ley K. Critical role of endothelial CXCR2 in LPS-induced neutrophil migration into the lung. The Journal of Clinical Investigation. 2006; 116:695–702. [PubMed: 16485040]

27. Wang L, Manji GA, Grenier JM, Al-Garawi A, Merriam S, Lora JM, Geddes BJ, Briskin M, DiStefano PS, Bertin J. PYPAF7, a novel PYRIN-containing Apaf1-like protein that regulates activation of NF-kappa B and caspase-1-dependent cytokine processing. J Biol Chem. 2002; 277:29874–29880. [PubMed: 12019269]

28. Williams KL, Taxman DJ, Linhoff MW, Reed W, Ting JP. Cutting edge: Monarch-1 : a pyrin/nucleotide-binding domain/leucine-rich repeat protein that controls classical and nonclassical MHC class I genes. J Immunol. 2003; 170:5354–5358. [PubMed: 12759408]

29. Hartmann BM, Li W, Jia J, Patil S, Marjanovic N, Martínez-Romero C, Albrecht RA, Hayot F, García-Sastre A, Wetmur JG, Moran TM, Sealfon SC. Mouse Dendritic Cell (DC) Influenza Virus Infectivity Is Much Lower than That for Human DCs and Is Hemagglutinin Subtype Dependent. J Virol. 2013; 87:1916–1918. [PubMed: 23192878]

30. Datta S, Biswas R, Novotny M, Pavicic PG Jr, Herjan T, Mandal P, Hamilton TA. Tristetraprolin regulates CXCL1 (KC) mRNA stability. J Immunol. 2008; 180:2545–2552. [PubMed: 18250465]

31. Hamilton T, Li X, Novotny M, Pavicic PG Jr, Datta S, Zhao C, Hartupee J, Sun D. Cell type- and stimulus-specific mechanisms for post-transcriptional control of neutrophil chemokine gene expression. J Leukoc Biol. 2012; 91:377–383. [PubMed: 22167720]

32. Herjan T, Yao P, Qian W, Li X, Liu C, Bulek K, Sun D, Yang WP, Zhu J, He A, Carman J, Erzurum S, Lipshitz H, Fox P, Hamilton T, Li X. HuR is required for IL-17-induced Act1-mediated CXCL1 and CXCL5 mRNA stabilization. J Immunol. 2013; 191:640–649. [PubMed: 23772036]

33. Thuraisingam T, Xu YZ, Moisan J, Lachance C, Garnon J, Di Marco S, Gaestel M, Radzioch D. Distinct role of MAPKAPK-2 in the regulation of TNF gene expression by Toll-like receptor 7 and 9 ligands. Mol Immunol. 2007; 44:3482–3491. [PubMed: 17485113]

34. Srivastava B, Blazejewska P, Hessmann M, Bruder D, Geffers R, Mauel S, Gruber AD, Schughart K. Host genetic background strongly influences the response to influenza a virus infections. PLoS One. 2009; 4:e4857. [PubMed: 19293935]

35. Ferris MT, Aylor DL, Bottomly D, Whitmore AC, Aicher LD, Bell TA, Bradel-Tretheway B, Bryan JT, Buus RJ, Gralinski LE, Haagmans BL, McMillan L, Miller DR, Rosenzweig E, Valdar W, Wang J, Churchill GA, Threadgill DW, McWeeney SK, Katze MG, Pardo-Manuel de Villena F, Baric RS, Heise MT. Modeling Host Genetic Regulation of Influenza Pathogenesis in the Collaborative Cross. PLoS Path. 2013; 9:e1003196.

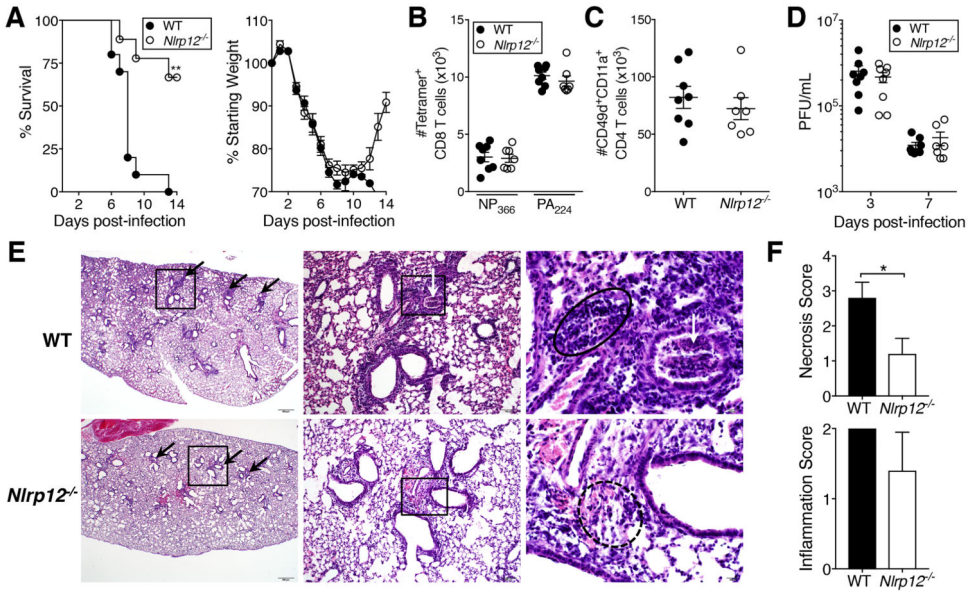

Figure 1. Improved survival of *Nlrp12*$^{-/-}$ mice following lethal IAV infection

(A) Mice were infected with a 4LD_{50} inoculum of IAV and monitored for survival and weight loss through day 14 post-infection. (B, C) Seven days post-infection, IAV-specific $CD8^+$ (B) and $CD4^+$ (C) T cells in the lungs were enumerated using indicated markers. (D) At days three and seven post-infection, virus was quantified in lung homogenate supernatants by plaque assay. (E) H&E-stained sections of lungs harvested five days post-infection. Scale bars and original magnification: left, 500μm (2×); middle, 100μm (10×); right, 20μm (50×). Boxes indicate the area magnified in the panel immediately to the right. Black arrows indicate peribronchiolar inflammation, white arrows indicate cellular debris within the airway, solid circle outlines lymphocytic infiltrates, dotted circle outlines scattered mixed inflammatory cells within the pulmonary interstitium. (F) Scoring of necrosis and inflammation in H&E stained lung sections. (A) Results are representative of two independent experiments, n=10 WT, 9 *Nlrp12*$^{-/-}$; (B-D) results are representative of two independent experiments, n= 6-8 per group; (E, F) results are representative of one experiment, n=5 per group, graphed as mean ± SD. *p<0.05, one sample t-test; **p<0.01, Gehan-Breslow-Wilcoxon test.

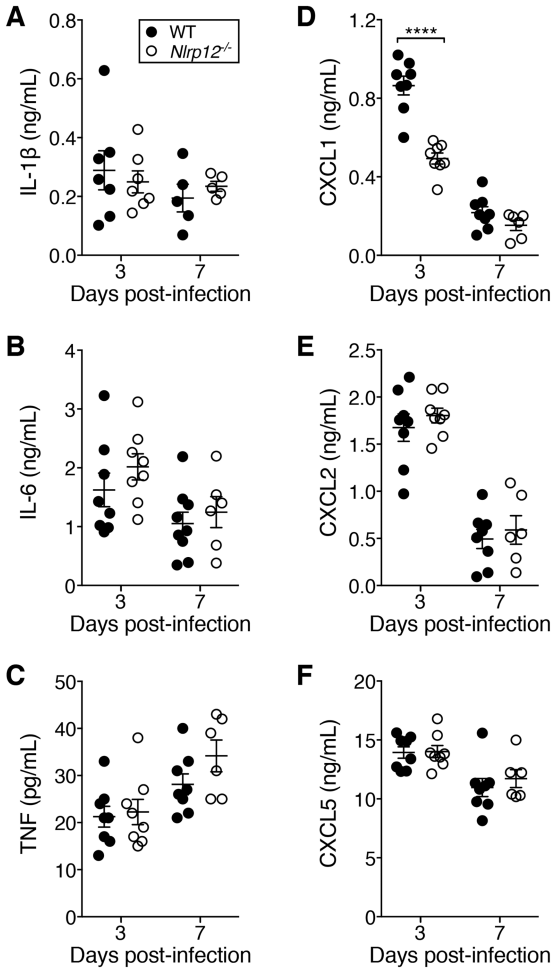

Figure 2. *Nlrp12*$^{-/-}$ mice have decreased pulmonary CXCL1 following lethal IAV infection

(A-F) Mice were infected with a 4LD_{50} inoculum of IAV and cytokines and chemokines were quantified by ELISA on lung homogenate supernatants. Data were pooled from two independent experiments, n=6-10 per group, error bars represent SEM. Data from individuals with IL-1β values below the limit of detection were not graphed. All cytokines and chemokines shown were below the limit of detection in lung homogenate supernatants from naïve mice. ****p<0.0001, ordinary one-way ANOVA with Sidak's multiple comparisons test.

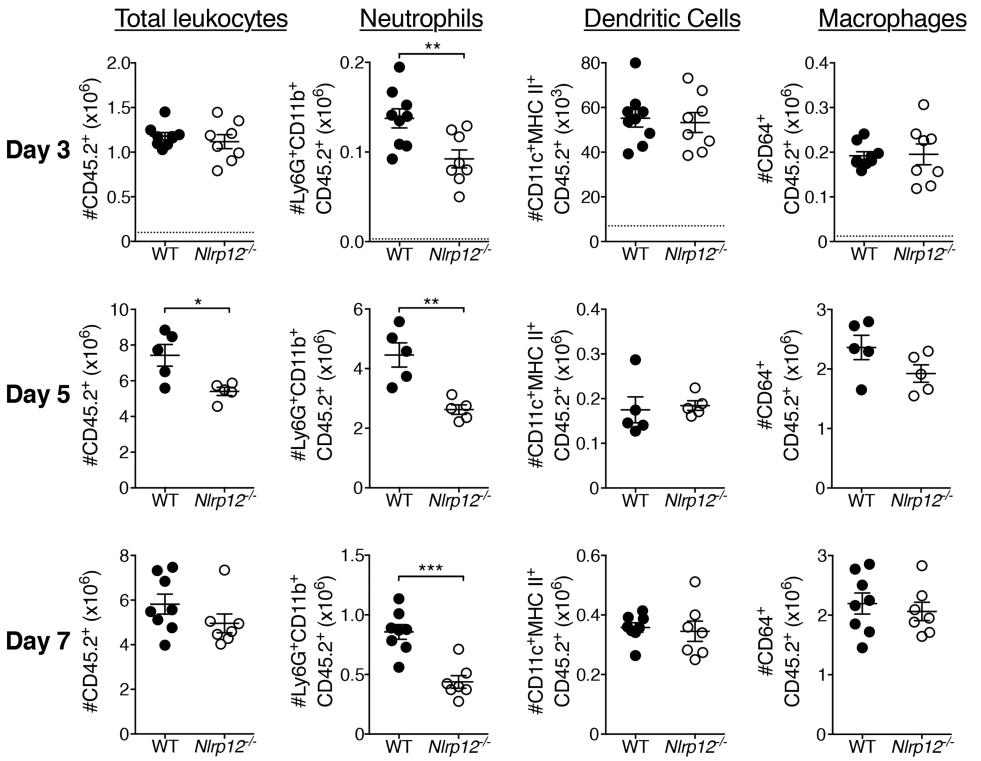

Figure 3. *Nlrp12*$^{-/-}$ mice have decreased pulmonary neutrophils during IAV infection

Mice were infected with a $4LD_{50}$ inoculum of IAV. Indicated cell populations in lungs were enumerated by flow cytometry at three, five, or seven days post infection, using gating described in Fig. S2A. Three and seven days: pooled from two independent experiments, n=7-9 per group. Five days: from one experiment, n=5 per group. Error bars represent SEM. *p<0.05, **p<0.01, ***p<0.001, student's t-test.

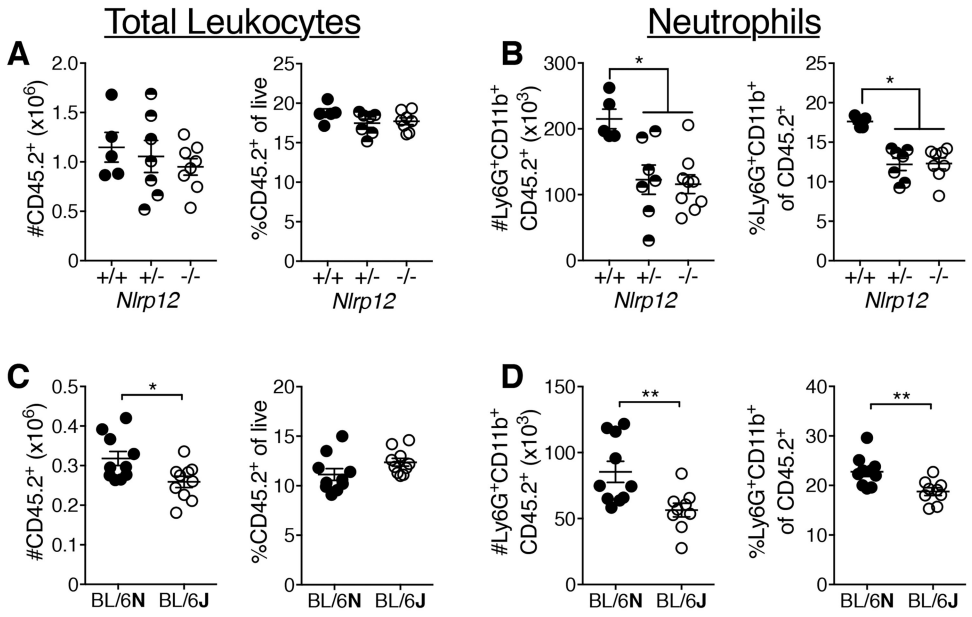

Figure 4. Diminished neutrophil recruitment in response to IAV in *Nrlp12*$^{-/-}$, *Nlrp12*$^{+/-}$, and C57BL/6J mice

Mice were infected with a $4LD_{50}$ inoculum of IAV. Indicated cell populations were enumerated in the lungs by flow cytometry at three days post -infection. (A, B) Data were pooled from two separate experiments, n=5-8 per group. (C, D) Data were pooled from two separate experiments, n=10 per group. Error bars represent SEM. *p<0.05, **p<0.01, student's t-test.

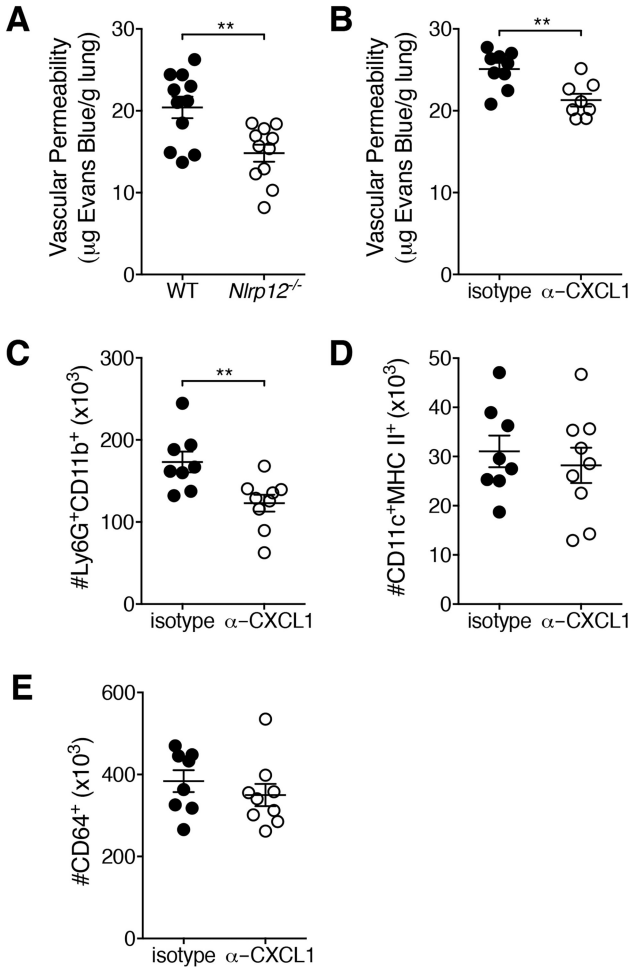

Figure 5. *Nlrp12*$^{-/-}$ mice have decreased pulmonary microvascular permeability

(A) Mice were infected with a 4LD_{50} inoculum of IAV. At day five post-infection, vascular permeability was measured by Evans blue extravasation. (B, C) On day 0 and day 3 of infection, mice were administered CXCL1 blocking antibody or isotype control antibody i.p. (C, E) Indicated cell populations were enumerated by flow cytometry. Data were pooled from two independent experiments, n=8-11 per group. Error bars represent SEM. **p<0.01, student's t-test.

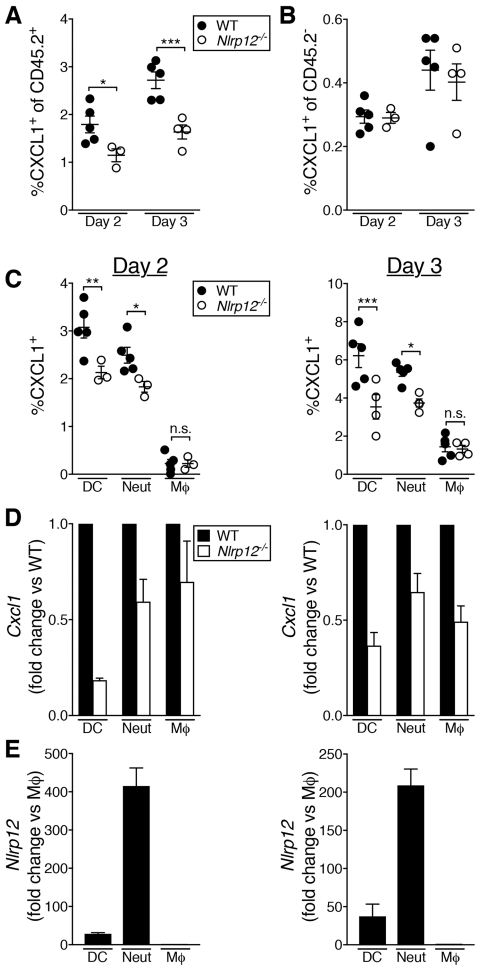

Figure 6. Decreased CXCL1 production by immune cells in the lungs of *Nlrp12*$^{-/-}$ mice during IAV infection

Mice were infected with a 4LD_{50} inoculum of IAV. (A-C) At the indicated day post-infection, $CXCL1^+$ cell populations were enumerated in the lungs by flow cytometry. (D, E) At the indicated day post-infection, cell populations were purified by FACS and gene expression was determined by qRT-PCR. (A-C) Results are representative of two independent experiments, n=3-5 per group, error bars represent SEM. (D, E) Data were pooled from two independent experiments, graphed as mean ± SEM * $p<0.05$, ** $p<0.01$, *** $p<0.001$, student's t-test.

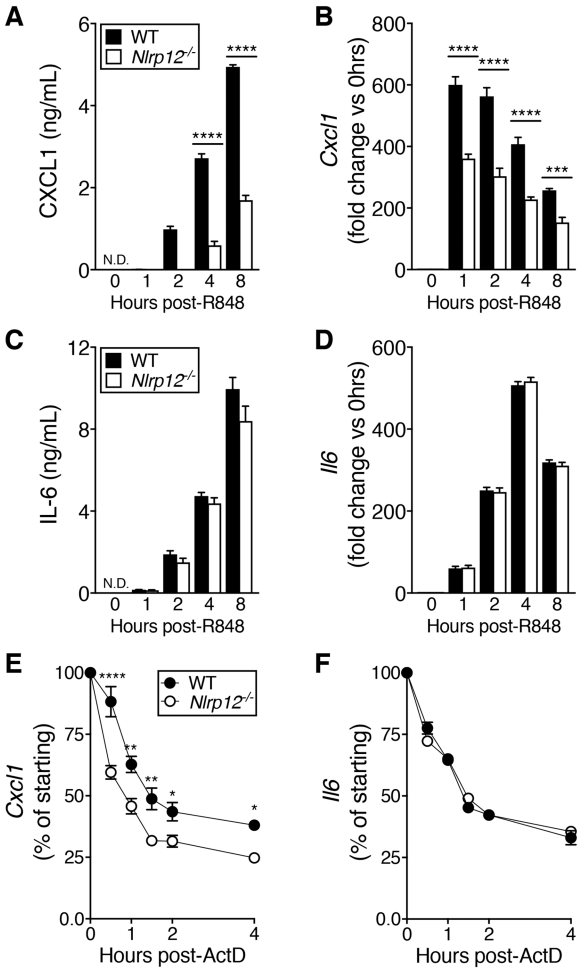

Figure 7. Decreased *Cxcl1* transcript stability in R848-stimulated *Nlrp12*$^{-/-}$ BMDCs

(A-D) BMDCs were treated with 1μg/mL R848 for the indicated amount of time and CXCL1 and IL-6 gene expression and protein were quantified. (E, F) BMDCs were treated with 1μg/mL R848 for 3hrs followed by the addition of ActD. At the indicated times after addition of ActD, RNA was extracted and qRT-PCR was used to quantify remaining *Cxcl1* or *Il6* transcripts. Results are presented as % transcript present immediately prior to ActD treatment (0hrs). (A-D) Data shown are representative of two independent experiments. (E, F) Data were pooled from three separate experiments. All data are graphed as mean ± SEM. *p<0.05, **p<0.01, ***p<0.001, ****p<0.0001, ordinary one-way ANOVA (A-D), two-way repeated measures ANOVA (E, F) with Sidak's multiple comparisons test (A-F).